

# Disodium Edetate As a Promising Interfacial Material for Inverted Organic Solar Cells and the Device Performance Optimization

Xiaodong Li,<sup>†,§</sup> Wenjun Zhang,<sup>†</sup> Xueyan Wang,<sup>†,§</sup> Feng Gao,<sup>\*,‡</sup> and Junfeng Fang<sup>\*,†</sup>

<sup>†</sup>Ningbo Institute of Materials and Technology and Engineering, Chinese Academy of Sciences, Ningbo 315201, China

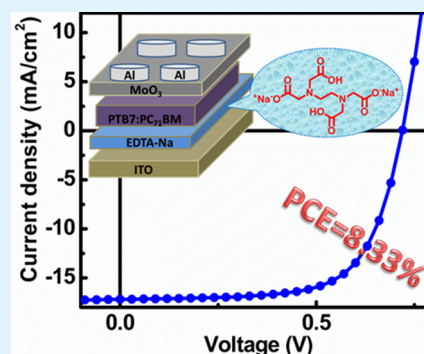
<sup>‡</sup>Biomolecular and Organic Electronics, Department of Physics, Chemistry and Biology (IFM), Linköping University, Linköping SE-581 83, Sweden

<sup>§</sup>University of Chinese Academy of Sciences, Beijing 100049, China

## Supporting Information

**ABSTRACT:** Disodium edetate (EDTA-Na), a popular hexadentate ligand in analytical chemistry, was successfully introduced in organic solar cells (OSCs) as cathode interfacial layer. The inverted OSCs with EDTA-Na showed superior performance both in power conversion efficiency and devices stability compared with conventional devices. Interestingly, we found that the performance of devices with EDTA-Na could be optimized through external bias treatment. After optimization, the efficiency of inverted OSCs with device structure of ITO/EDTA-Na/polymer thieno[3,4-*b*]thiophene/benzodithiophene (PTB7):PC<sub>71</sub>BM/MoO<sub>3</sub>/Al was significantly increased to 8.33% from an initial value of 6.75%. This work introduces a new class of interlayer materials, small molecule electrolytes, for organic solar cells.

**KEYWORDS:** small molecule electrolytes, interlayer, organic solar cells, external bias



Organic solar cells (OSCs) have attracted substantial interest for several reasons, such as low-cost, flexibility and roll-to-roll fabrication compared with conventional silicon-based solar cells.<sup>1–3</sup> Initially, OSCs employed a so-called conventional configuration, where the poly(3,4-ethylenedioxythiophene):(polystyrene sulfonic acid) (PEDOT:PSS) modified indium tin oxide (ITO) was used as the anode and low work function (WF) metals (Ba or Ca) used as the cathode.<sup>1,4</sup> Though relatively high power conversion efficiency (PCE) (7%–8%) was obtained using the conventional device structure,<sup>5–8</sup> rapid degradation of the device performance was an inevitable problem because of easy oxidation of low WF metals as well as the acid nature of PEDOT:PSS.

Compared with conventional OSCs, inverted OSCs (i-OSCs) showed much better stability because of the employment of high WF metals (Al or Ag) as the hole collection anode. To obtain high performance i-OSCs, it is of critical importance to modify the WF of ITO so that it could be employed to effectively collect electrons.<sup>9</sup> And much work has been focused on this research direction. For example, n-type metal oxides, such as zinc oxide (ZnO)<sup>10</sup> and titanium oxide (TiOx),<sup>11,12</sup> have been successfully applied in efficient i-OSCs due to their favorable electron transport properties. However, these metal oxides usually need an extra post-treatment, like high temperature, to promote crystallization<sup>12,13</sup> or UV-irradiation<sup>14</sup> to change the interfacial chemical states, which is incompatible with low-cost large-scale production.

Alternatively, organic interfacial materials also attract much interest in i-OSCs and polymer light-emitting diodes (PLEDs)

because of their easy solution processability and low temperature treatment.<sup>15–20</sup> Among others, water/alcohol-soluble conjugated polymers (WSCPs) demonstrate successful applications in i-OSCs.<sup>21,22</sup> These interfacial materials could effectively adjust the WF of ITO by forming an interfacial dipole between ITO and the active layer, benefiting charge transport. However, they usually suffer from the difficulty of synthesis and purification because of the complex C–C coupling and polymerization compared with small molecule electrolytes (SMEs).<sup>18,23</sup> Despite obvious advantages of SMEs compared with WSCPs, the SMEs generally could not work as well as WSCPs, and the reason is not clear yet.<sup>21,23,24</sup>

Here, we demonstrate that a SME (EDTA-Na, Figure 1) without any  $\pi$ -delocalized groups can also work well as an

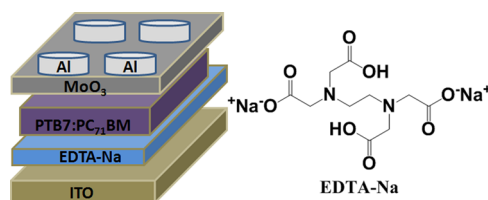


**Figure 1.** Device configuration and structure of EDTA-Na used in our work.

Received: July 8, 2014

Accepted: November 17, 2014

Published: November 17, 2014

efficient interlayer material in i-OSCs. We can optimize the performance of i-OSCs with the EDTA-Na interlayer using an external bias treatment. We demonstrate that the power conversion efficiency (PCE) based on PTB7:PC<sub>71</sub>BM could be increased from ~6% to over 8% after optimization, which further confirmed our previous studies about the excellent electrons transport property for materials without any  $\pi$ -delocalized groups.<sup>18</sup> The external bias might promote the molecule orientation or motion to form an interfacial dipole.<sup>25–27</sup> As a result, the interface recombination was effectively reduced, leading to an improved fill factor (FF) and open-circuit voltage ( $V_{oc}$ ).

To effectively modify the ITO electrode, we spin-coated the EDTA-Na solution of 3 mg/mL in water on ITO glass at 4000 rpm for 60 s, forming some islandlike structures on ITO surface as observed from SEM images (see Figure S1 in the Supporting Information). After modified by EDTA-Na interlayer, the work function (WF) of ITO could be regulated from 4.8 to 4.0 eV, making the ITO electrode more suitable for electron collection (calculated from UPS in Figure S2 in the Supporting Information). When introducing EDTA-Na in to OSCs based on PTB7:PC<sub>71</sub>BM systems, initially, the as-prepared devices exhibited moderate performance with a  $V_{oc}$  of 0.638 V and FF of 60.7%, indicating the moderated function of EDTA-Na layer. Interestingly, when we repeated the measurement, the  $V_{oc}$  and FF increased to 0.665 V and 62.1%, respectively (Table 1). The

**Table 1. Photovoltaic Parameters of a Conventional Device and Devices with EDTA-Na (3 mg/mL) Measured under Different Conditions with a Scan Range from 1.5 V to -1.5 V**

	$V_{oc}$ (V)	$J_{sc}$ (mA/cm <sup>2</sup> )	FF (%)	PCE (%)	
conventional	0.681	16.16	64.6	7.11	
EDTA-Na repeated measurement	0.638	15.75	60.7	6.10	1 <sup>a</sup>
	0.665	15.76	62.1	6.50	2 <sup>a</sup>
	0.681	15.76	63.1	6.76	3 <sup>a</sup>
	0.692	15.77	63.7	6.95	4 <sup>a</sup>
	0.698	15.78	64.3	7.08	5 <sup>a</sup>
EDTA-Na, +2 V bias, different bias time	0.643	17.14	61.3	6.75	0 s <sup>b</sup>
	0.696	17.18	64.7	7.74	30 s <sup>b</sup>
	0.709	17.18	66.1	8.05	60 s <sup>b</sup>
	0.716	17.18	66.8	8.22	90 s <sup>b</sup>
	0.720	17.18	67.4	8.33	120 s <sup>b</sup>

<sup>a</sup>Times of measurement under scan range of -1.5–1.5 V. <sup>b</sup>Time of +2 V bias applied on devices.

$V_{oc}$  and FF kept increasing with increasing times of measurements. And after 5 times of measurement, the  $V_{oc}$  and FF increased to 0.698 V and 64.3%, respectively. As a result, the PCE increased from 6.10% to 7.08% (shown in Figure 2a).

Because an external scan bias (-1.5 V–1.5 V) was applied on the device during measurements, this external bias might affect the EDTA-Na property or the interface of ITO/EDTA-Na, resulting in the device performance enhancement. To examine this possibility, we directly applied a constant bias on the device before the measurement and investigated the effect of the bias on the device performance. And to avoid the effect of repeated measurements on device performance as possible, all the constant bias was applied on separated as-prepared devices. As shown in Figure 2b, the as-prepared devices showed moderate  $V_{oc}$  of 0.656 V. When a negative bias (-4 V for 5s,

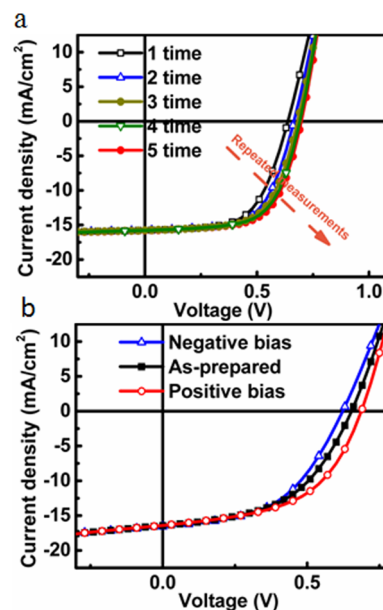


**Figure 2.** (a) Comparison of  $J$ - $V$  curve for the as-prepared device and that after repeated measurements under the scan range from 1.5 V to -1.5 V. (b) Device performance after positive (+4 V) and negative (-4 V) bias.

corresponding to Al electrode) was applied, the  $V_{oc}$  could be decreased to 0.615 V, whereas if a positive bias (+4 V for 5s) was applied, both  $V_{oc}$  (from 0.656 to 0.686 V) and FF (from 54.2 to 60.8%) increased, leading to the improved PCE from 5.75 to 6.70%. This experiment indicated that the positive bias plays a major role in the performance improvement during the repeated measurements, whereas the effect of negative bias is negligible.

To further investigate the effect of the external bias on device performance, we systematically examine the relation between the bias time and device performance (Figure 3a). The as-prepared device showed a moderate PCE of 6.75% with a  $V_{oc}$  of 0.643 V and FF of 61.3%. When a 2 V bias was applied for 30s, the PCE significantly increased to 7.74%, mainly due to the much improved  $V_{oc}$  (0.696 V) and FF of (64.7%). And when the bias time extended to 60 s, the PCE could further increase to 8.05%, with  $V_{oc}$  of 0.709 V and FF of 66.1%, although the increasing rate was a little decreased. If the bias time was further increased, the device parameters tended to saturate gradually, as shown in Table 1. After the 2 V bias was applied for 120s, a  $V_{oc}$  of 0.720 V and FF of 67.4% were obtained, leading to a PCE of 8.33%. The specific devices parameter comparison before and after bias treatment was shown in Figure S3 in the Supporting Information. And if we increased the external bias to 4 V, much shorter time was needed to optimize the device performance. The PCE could be increased to 8.13% only after 20 s treatment of 4 V bias (see Figure S4 in the Supporting Information). Meanwhile, for conventional devices, there were almost no changes in device performance after external bias treatment, as shown in Figure S5 in the Supporting Information, indicating that the dependence of external bias treatment was mainly due to the existence of EDTA-Na interlayer. In addition, we also introduced a neutral polyfluorene derivative (PFN4) synthesized by our lab to replace ionic EDTA-Na layer for comparison and checked whether the beneficial bias effect still exist (see Figure S6 in the Supporting Information). The as-prepared devices with PFN4 showed a comparable PCE of 8.40% and

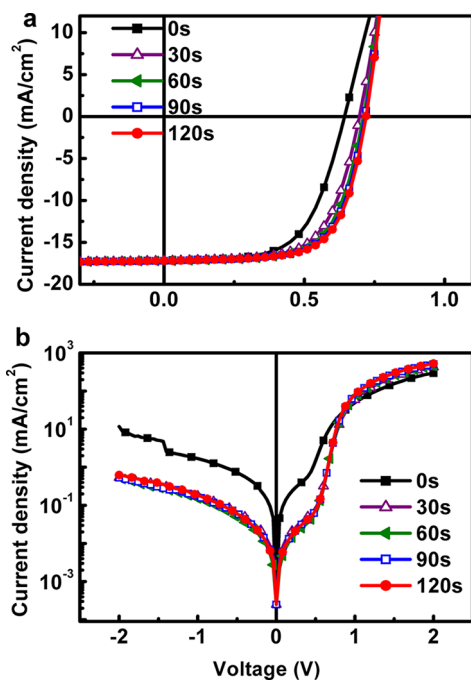


**Figure 3.** (a)  $J$ - $V$  curves for devices under +2 V bias for different time. (b)  $J$ - $V$  curves in dark conditions corresponding to a.

almost no changes in device performance were observed when 2 V bias was applied (similar to that observed in conventional devices shown in Figure S5 in the Supporting Information), which may further indicate the existence of ions motion in EDTA-Na on the other side. On the other hand, we also investigated the real-time variation of current density (dark conditions) versus time when a positive bias was applied (see Figure S7 in the Supporting Information). The current density gradually decreased first and then slowly increased, which was very similar to the phenomenon observed in light-emitting electrochemical cells (LECs).<sup>28</sup> In LECs, the formation of electric double layer caused by ions motion successfully explained this current density variation.<sup>28</sup> In our devices, the ions motion in EDTA-Na under external bias might lead to the ions redistribution, forming interfacial dipole and decreasing the electron transport barrier.<sup>25–27</sup> And if we decreased the thickness of EDTA-Na (1 mg/mL), the improvement of  $V_{oc}$  and FF after 2 V bias treatment still existed (see Table S1 in the Supporting Information), whereas for the device with a thicker EDTA-Na interlayer (10 mg/mL), after 2 V bias treatment, the  $J_{sc}$  also greatly increased besides the improvement of  $V_{oc}$  and FF (see Table S2 in the Supporting Information). The EDTA-Na layer of 10 mg/mL was too thick for electrons to be transported, leading to the much low  $J_{sc}$  for as-prepared devices. After 2 V bias treatment, the introduction of interfacial dipole because of the ion redistribution may greatly decrease the transport barrier, thus improving the  $J_{sc}$  as well as the  $V_{oc}$  and FF.

In addition, the effect of external bias on  $J$ - $V$  curves under dark conditions was also studied. As shown in Figure 3b, the device after bias showed much lower leakage current compared with the as-prepared device, implying that the cathode interface (ITO/EDTA-Na, 3 mg/mL) became more beneficial for electron transport and hole blocking.<sup>29</sup> Moreover, the device after bias also showed larger injection current compared with the as-prepared device, indicating decreased series resistance for

electron injection from ITO/EDTA-Na cathode.<sup>30</sup> As a result, the suppressed leakage current and reduced series resistance for the devices after bias was favorable of a higher  $V_{oc}$  agreeing with the  $J$ - $V$  curves under solar simulation.

At last, we also studied the lifetime of devices with EDTA-Na (3 mg/mL) interlayer after bias treatment (all the devices were stored in glovebox filled with Ar without encapsulation). As shown in Figure 4, all the device parameters for EDTA-Na

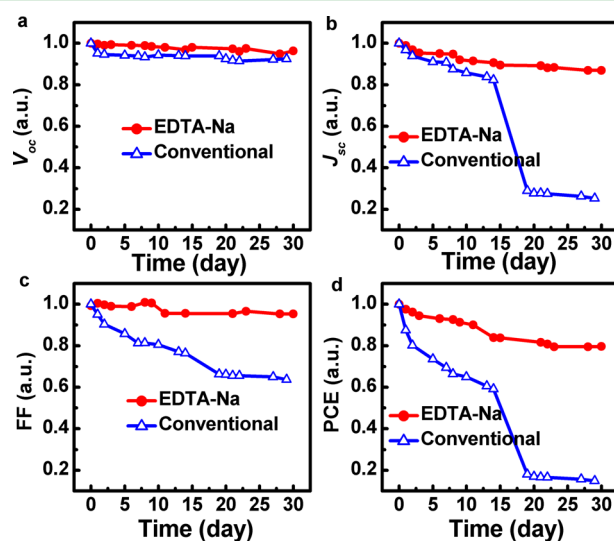


**Figure 4.** Decay of  $V_{oc}$ ,  $J_{sc}$ , FF, and PCE for inverted devices with EDTA-Na (3 mg/mL) and conventional devices.

interlayer exhibited much lower decay rate than that of conventional devices, especially for  $J_{sc}$  and FF (Figure 4b, c). As a result, 80% of the PCE for EDTA-Na devices could still be maintained even after storage for 30 days, whereas for conventional devices, only about 15% of the performance still existed, indicating that EDTA-Na interlayer not only improved the device efficiency (statistical analysis is shown in Figure S8 in the Supporting Information) but also increased the device stability effectively. Note that in EDTA-Na devices, only 4% of the  $V_{oc}$  and FF decayed after 30 days. Considering that for as-prepared EDTA-Na devices, the performance improvement after bias treatment was mainly due to the increase of  $V_{oc}$  and FF (Table 1), it seemed reasonable to believe that the beneficial effect of bias treatment could be well maintained within a period of time. To further investigate the bias effect on device performance, we stored the bias treatment devices ( $V_{oc}$  of 0.731 V, PCE of 8.06%) in glovebox for 20 h, the device exhibited a PCE of 7.26% with  $V_{oc}$  of 0.718 V, which is still much better than the as-prepared device performance ( $V_{oc}$  of 0.637 V and PCE of 5.74%), further indicating the well maintenance of the bias effect. However, if we applied a 2 V bias for 120 s, the PCE could slightly recover to 7.86% with a  $V_{oc}$  of 0.731 V, which may be caused by the ion relaxation and redistribution.

In conclusion, we successfully introduced SME interlayer (EDTA-Na) into i-OSCs (based on PTB7:PC<sub>71</sub>BM) and found that external bias could help to optimize the device performance. By applying a 2 V bias for 120 s, the PCE could be significantly improved from 6.75 to 8.33%, mainly because of the enhanced  $V_{oc}$  and FF. Our work indicated that the SMEs without any  $\pi$ -delocalized groups could also be an excellent cathode interfacial material after reasonable optimization; on the other hand, it indicated the critical role of the external bias

on i-OSCs with SMEs, and further investigation is ongoing to understand the mechanisms behind it.

## ■ ASSOCIATED CONTENT

### ● Supporting Information

Experimental section, Figure S1–S9, and Table S1–S2. This material is available free of charge via the Internet at <http://pubs.acs.org/>.

## ■ AUTHOR INFORMATION

### Corresponding Authors

\*E-mail: [fangjf@nimte.ac.cn](mailto:fangjf@nimte.ac.cn).

\*E-mail: [fenga@ifm.liu.se](mailto:fenga@ifm.liu.se).

### Notes

The authors declare no competing financial interest.

## ■ ACKNOWLEDGMENTS

This project (61474125, 51273208) was supported by National Natural Science Foundation of China and Zhejiang Provincial Natural Science Foundation of China (LR14E030002). The work was also supported by Hundred Talent Program of Chinese Academy of Sciences, the Ningbo Natural Science Foundation of China (2012A610114; 2013A610132). F.G. acknowledges the financial support of the European Commission under a Marie Curie Intra-European Fellowship for Career Development.

## ■ REFERENCES

- (1) Yu, G.; Gao, J.; Hummelen, J.; Wudl, F.; Heeger, A. J. Polymer Photovoltaic Cells: Enhanced Efficiencies via a Network of Internal Donor-acceptor Heterojunctions. *Science* **1995**, *1789*–1790.
- (2) Günes, S.; Neugebauer, H.; Sariciftci, N. S. Conjugated Polymer-Based Organic Solar Cells. *Chem. Rev.* **2007**, *107*, 1324–1338.
- (3) Li, G.; Zhu, R.; Yang, Y. Polymer Solar Cells. *Nat. Photonics* **2012**, *6*, 153–161.
- (4) Li, X.; Zhang, W.; Wu, Y.; Min, C.; Fang, J. Solution-Processed MoS<sub>x</sub> as an Efficient Anode Buffer Layer in Organic Solar Cells. *ACS Appl. Mater. Interfaces* **2013**, *5*, 8823–8827.
- (5) Chen, H.-Y.; Hou, J.; Zhang, S.; Liang, Y.; Yang, G.; Yang, Y.; Yu, L.; Wu, Y.; Li, G. Polymer Solar Cells with Enhanced Open-circuit Voltage and Efficiency. *Nat. Photonics* **2009**, *3*, 649–653.
- (6) Liang, Y.; Xu, Z.; Xia, J.; Tsai, S.-T.; Wu, Y.; Li, G.; Ray, C.; Yu, L. For the Bright Future—Bulk Heterojunction Polymer Solar Cells with Power Conversion Efficiency of 7.4%. *Adv. Mater.* **2010**, *22*, E135–E138.
- (7) van der Poll, T. S.; Love, J. A.; Nguyen, T.-Q.; Bazan, G. C. Non-Basic High-Performance Molecules for Solution-Processed Organic Solar Cells. *Adv. Mater.* **2012**, *24*, 3646–3649.
- (8) Zhou, J.; Zuo, Y.; Wan, X.; Long, G.; Zhang, Q.; Ni, W.; Liu, Y.; Li, Z.; He, G.; Li, C.; Kan, B.; Li, M.; Chen, Y. Solution-Processed and High-Performance Organic Solar Cells Using Small Molecules with a Benzodithiophene Unit. *J. Am. Chem. Soc.* **2013**, *135*, 8484–8487.
- (9) Chen, L.-M.; Xu, Z.; Hong, Z.; Yang, Y. Interface Investigation and Engineering - Achieving High Performance Polymer Photovoltaic Devices. *J. Mater. Chem.* **2010**, *20*, 2575–2598.
- (10) Sun, Y.; Seo, J. H.; Takacs, C. J.; Seifert, J.; Heeger, A. J. Inverted Polymer Solar Cells Integrated with a Low - Temperature - Annealed Sol - Gel - Derived ZnO Film as an Electron Transport Layer. *Adv. Mater.* **2011**, *23*, 1679–1683.
- (11) Tan, Z. a.; Zhang, W.; Zhang, Z.; Qian, D.; Huang, Y.; Hou, J.; Li, Y. High-Performance Inverted Polymer Solar Cells with Solution-Processed Titanium Chelate as Electron-Collecting Layer on ITO Electrode. *Adv. Mater.* **2012**, *24*, 1476–1481.
- (12) Tao, C.; Ruan, S.; Zhang, X.; Xie, G.; Shen, L.; Kong, X.; Dong, W.; Liu, C.; Chen, W. Performance Improvement of Inverted Polymer

Solar Cells with Different Top Electrodes by Introducing a MoO<sub>3</sub> Buffer Layer. *Appl. Phys. Lett.* **2008**, *93*, 193307–1–193307–3.

- (13) Kyaw, A.; Sun, X.; Jiang, C.; Lo, G.; Zhao, D.; Kwong, D. An Inverted Organic Solar Cell Employing a Sol-gel Derived ZnO Electron Selective Layer and Thermal Evaporated MoO<sub>3</sub> Hole Selective Layer. *Appl. Phys. Lett.* **2008**, *93*, 221107–221107–3.

- (14) Kim, J.; Kim, G.; Choi, Y.; Lee, J.; Heum Park, S.; Lee, K. Light-soaking Issue in Polymer Solar Cells: Photoinduced Energy Level Alignment at the Sol-gel Processed Metal Oxide and Indium Tin Oxide Interface. *J. Appl. Phys.* **2012**, *111*, 114511–1–114511–9.

- (15) Yang, R.; Xu, Y.; Dang, X.-D.; Nguyen, T.-Q.; Cao, Y.; Bazan, G. C. Conjugated Oligoelectrolyte Electron Transport/Injection Layers for Organic Optoelectronic Devices. *J. Am. Chem. Soc.* **2008**, *130*, 3282–3283.

- (16) Fang, J.; Wallikewitz, B. H.; Gao, F.; Tu, G.; Müller, C.; Pace, G.; Friend, R. H.; Huck, W. T. S. Conjugated Zwitterionic Polyelectrolyte as the Charge Injection Layer for High-Performance Polymer Light-Emitting Diodes. *J. Am. Chem. Soc.* **2010**, *133*, 683–685.

- (17) Duan, C.; Wang, L.; Zhang, K.; Guan, X.; Huang, F. Conjugated Zwitterionic Polyelectrolytes and Their Neutral Precursor as Electron Injection Layer for High-Performance Polymer Light-Emitting Diodes. *Adv. Mater.* **2011**, *23*, 1665–1669.

- (18) Min, C.; Shi, C.; Zhang, W.; Jiu, T.; Chen, J.; Ma, D.; Fang, J. A Small-Molecule Zwitterionic Electrolyte without a  $\pi$ -Delocalized Unit as a Charge-Injection Layer for High-Performance PLEDs. *Angew. Chem., Int. Ed.* **2013**, *52*, 3417–3420.

- (19) Zilberberg, K.; Behrendt, A.; Kraft, M.; Scherf, U.; Riedl, T. Ultrathin Interlayers of a Conjugated Polyelectrolyte for Low Work-function Cathodes in Efficient Inverted Organic Solar Cells. *Org. Electron.* **2013**, *14*, 951–957.

- (20) Wang, F.; Xiong, T.; Qiao, X.; Ma, D. Origin of Improvement in Device Performance via the Modification Role of Cesium Hydroxide Doped Tris(8-hydroxyquinoline) Aluminum Interfacial Layer on ITO Cathode in Inverted Bottom-emission Organic Light-emitting Diodes. *Org. Electron.* **2009**, *10*, 266–274.

- (21) He, Z.; Wu, H.; Cao, Y. Recent Advances in Polymer Solar Cells: Realization of High Device Performance by Incorporating Water/Alcohol-Soluble Conjugated Polymers as Electrode Buffer Layer. *Adv. Mater.* **2014**, *26*, 1006–1024.

- (22) Duan, C.; Zhang, K.; Zhong, C.; Huang, F.; Cao, Y. Recent Advances in Water/alcohol-Soluble  $\pi$ -conjugated Materials: New Materials and Growing Applications in Solar Cells. *Chem. Soc. Rev.* **2013**, *42*, 9071–9104.

- (23) Wu, C.-H.; Chin, C.-Y.; Chen, T.-Y.; Hsieh, S.-N.; Lee, C.-H.; Guo, T.-F.; Jen, A. K. Y.; Wen, T.-C. Enhanced Performance of Polymer Solar Cells Using Solution-processed Tetra-n-alkyl Ammonium Bromides as Electron Extraction Layers. *J. Mater. Chem. A* **2013**, *1*, 2582–2587.

- (24) He, Z.; Zhong, C.; Su, S.; Xu, M.; Wu, H.; Cao, Y. Enhanced Power-conversion Efficiency in Polymer Solar Cells Using an Inverted Device Structure. *Nat. Photonics* **2012**, *6*, 591–595.

- (25) Hoven, C.; Yang, R.; Garcia, A.; Heeger, A. J.; Nguyen, T.-Q.; Bazan, G. C. Ion Motion in Conjugated Polyelectrolyte Electron Transporting Layers. *J. Am. Chem. Soc.* **2007**, *129*, 10976–10977.

- (26) Lee, B. H.; Jung, I. H.; Woo, H. Y.; Shim, H.-K.; Kim, G.; Lee, K. Polyelectrolytes: Multi-Charged Conjugated Polyelectrolytes as a Versatile Work Function Modifier for Organic Electronic Devices. *Adv. Funct. Mater.* **2014**, *24*, 1029–1029.

- (27) Chen, L.; Xie, C.; Chen, Y. Self-Assembled Conjugated Polyelectrolyte–Ionic Liquid Crystal Complex as an Interlayer for Polymer Solar Cells: Achieving Performance Enhancement via Rapid Liquid Crystal-Induced Dipole Orientation. *Macromolecules* **2014**, *47*, 1623–1632.

- (28) Van Reenen, S.; Matyba, P.; Dzwilewski, A.; Janssen, R. A. J.; Edman, L.; Kemerink, M. A Unifying Model for the Operation of Light-Emitting Electrochemical Cells. *J. Am. Chem. Soc.* **2010**, *132*, 13776–13781.

(29) Li, X.; Zhang, W.; Wu, Y.; Min, C.; Fang, J. High Performance Polymer Solar Cells With a Polar Fullerene Derivative as the Cathode Buffer Layer. *J. Mater. Chem. A* **2013**, *1*, 12413–12416.

(30) Duan, C.; Zhong, C.; Liu, C.; Huang, F.; Cao, Y. Highly Efficient Inverted Polymer Solar Cells Based on an Alcohol Soluble Fullerene Derivative Interfacial Modification Material. *Chem. Mater.* **2012**, *24*, 1682–1689.